Article:

Bajpai, A, Aslam, Z, Hampel, S et al. (2 more authors) (2017) A carbon-nanotube based nano-furnace for in-situ restructuring of a magnetoelectric oxide. Carbon, 114. pp. 291-300. ISSN 0008-6223

https://doi.org/10.1016/j.carbon.2016.12.008

Accepted Manuscript

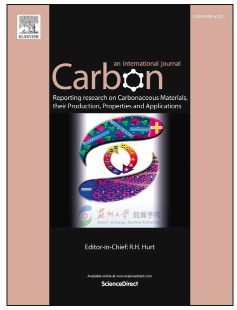

A carbon-nanotube based nano-furnace for *in-situ* restructuring of a magnetoelectric oxide

Ashna Bajpai, Zabeada Aslam, Silke Hampel, Ruediger Klingeler, Nicole Grobert

PII: S0008-6223(16)31077-6

DOI: 10.1016/j.carbon.2016.12.008

Reference: CARBON 11531

To appear in: *Carbon*

Received Date: 5 September 2016

Revised Date: 20 November 2016

Accepted Date: 2 December 2016

A carbon-nanotube based nano-furnace for *in-situ* restructuring of a magnetoelectric oxide

Ashna Bajpai[a]*, *Zabeada Aslam*[b], *Silke Hampel*[c], *Ruediger Klingeler*[d,e] *and Nicole Grobert*[f]

[a]Division of Physics and Center for Energy Science, Indian Institute of Science Education and Research (IISER), Pune, 411008, India.

[b]Institute for Materials Research School for Chemical and Process Engineering, University of Leeds, UK.

[c]Leibniz-Institute for Solid State and Materials Research, IFW Dresden - 01171 Dresden, Germany.

[d]Kirchhoff Institute of Physics, Heidelberg University, INF 227, 69120 Heidelberg, Germany.
[e]Centre for Advanced Materials, Heidelberg University, INF 225, 69120 Heidelberg, Germany.

[f]Department of Materials, University of Oxford, Parks Road, Oxford OX1 3PH, UK.

Abstract

We present current-voltage (I-V) characteristics of an individual carbon nanotube (CNT) filled with Cr_2O_3, a multi-functional magnetic oxide relevant to spintronics. We demonstrate that a filled CNT during a two probe I-V scan in suspended geometry, can be used like a nano-furnace for controlled restructuring of the oxide encapsulate. With proper utilization of Joule heating during I-V scans, the encapsulate, initially in the form of a polycrystalline nano-wire, converts to beads, nano-crystals and sheets within the CNT. These morphological phases are formed and preserved by controlling the amplitude, rate and holding time of the bias voltage. The sequential restructuring, observed in real time by Transmission Electron Microscopy (TEM), is also accompanied by a substantial enhancement in the current flowing through the CNT. We further demonstrate that advantageously tailoring the morphology of the encapsulate is linked to this current enhancement and can be a route for heat dissipation in nano devices. Magnetization measurements reveal that Cr_2O_3, a well known antiferromagnetic and magnetoelectric, when confined within CNT, exhibits logarithmic time dependence. This slow magnetization dynamics is associated to a pinning mechanism that points towards the possibility of stress induced moments in this system. These measurements elucidate novel magnetic properties of the encapsulate.

**Corresponding author. Tel +91-20-2590-8107. E mail : ashna@iiserpune.ac.in*

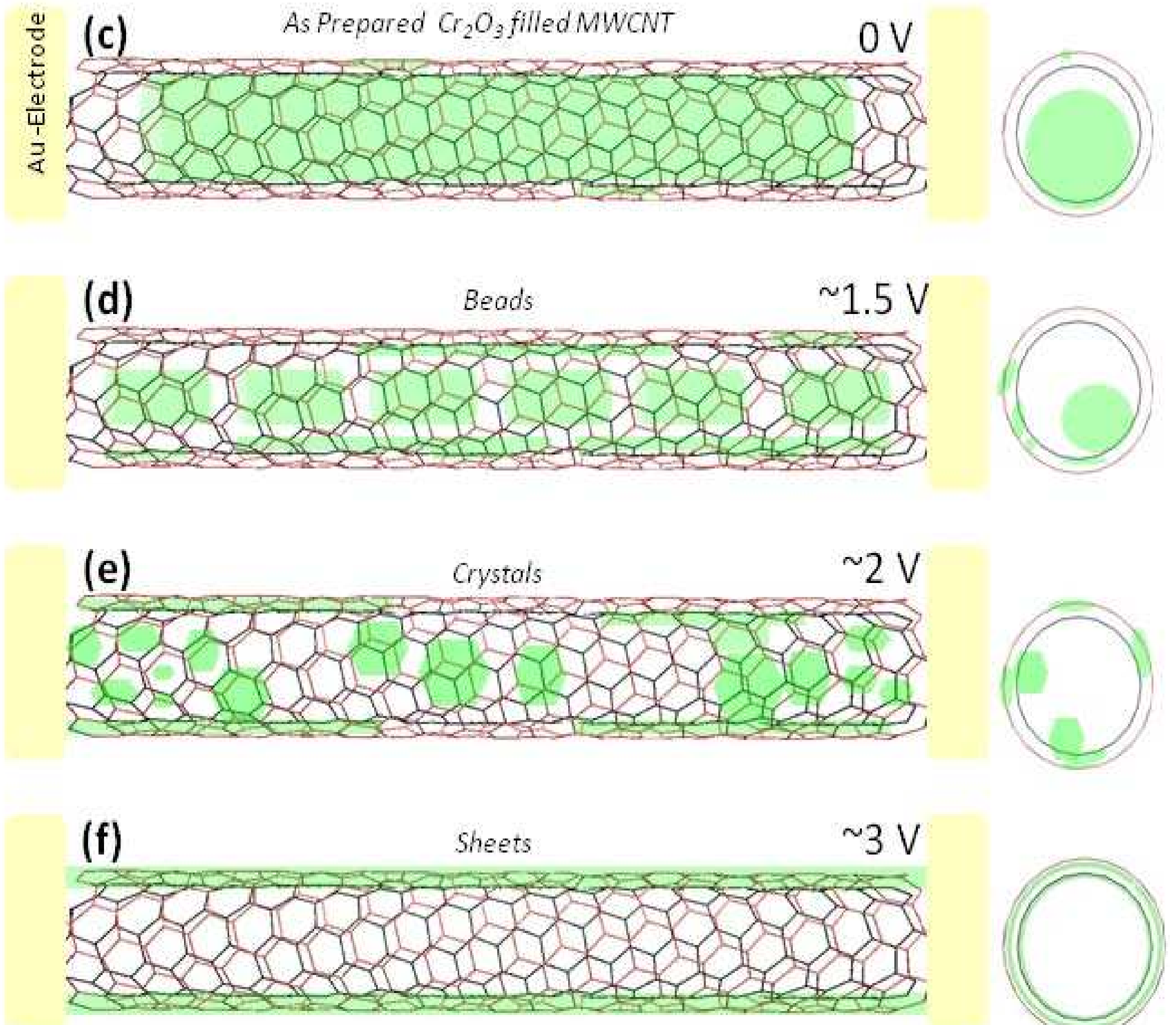
Au-Electrode
(c)
As Prepared Cr_2O_3 filled MWCNT
0 V
(d)
Beads
~1.5 V
(e)
Crystals
~2 V
(f)
Sheets
~3 V

A carbon-nanotube based nano-furnace for *in-situ* restructuring of a magnetoelectric oxide

Ashna Bajpai[a], Zabeada Aslam[b], Silke Hampel[c], Ruediger Klingeler[d,e] and Nicole Grobert[f]*

[a]Division of Physics and Center for Energy Science, Indian Institute of Science Education and Research (IISER), Pune, 411008, India.

[b]Institute for Materials Research School for Chemical and Process Engineering, University of Leeds, UK.

[c]Leibniz-Institute for Solid State and Materials Research, IFW Dresden - 01171 Dresden, Germany.

[d]Kirchhoff Institute of Physics, Heidelberg University, INF 227, 69120 Heidelberg, Germany.
[e]Centre for Advanced Materials, Heidelberg University, INF 225, 69120 Heidelberg, Germany.

[f]Department of Materials, University of Oxford, Parks Road, Oxford OX1 3PH, UK.

Abstract

We present current-voltage (I-V) characteristics of an individual carbon nanotube (CNT) filled with Cr_2O_3, a multi-functional magnetic oxide relevant to spintronics. We demonstrate that a filled CNT during a two probe I-V scan in suspended geometry, can be used like a nano-furnace for controlled restructuring of the oxide encapsulate. With proper utilization of Joule heating during I-V scans, the encapsulate, initially in the form of a polycrystalline nano-wire, converts to beads, nano-crystals and sheets within the CNT. These morphological phases are formed and preserved by controlling the amplitude, rate and holding time of the bias voltage. The sequential restructuring, observed in real time by Transmission Electron Microscopy (TEM), is also accompanied by a substantial enhancement in the current flowing through the CNT. We further demonstrate that advantageously tailoring the morphology of the encapsulate is linked to this current enhancement and can be a route for heat dissipation in nano devices. Magnetization measurements reveal that Cr_2O_3, a well known antiferromagnetic and magnetoelectric, when confined within CNT, exhibits logarithmic time dependence. This slow magnetization dynamics is associated to a pinning mechanism that points towards the possibility of stress induced moments in this system. These measurements elucidate novel magnetic properties of the encapsulate.

*Corresponding author. Tel +91-20-2590-8107. E mail : ashna@iiserpune.ac.in

1. Introduction

Probing the I-V characteristics of individual carbon nanotubes[1-15] has been a subject of intense investigations since it is crucial for their integration into miniaturized devices. Such I-V measurements[1-5] are central to the utility of the CNT, either as superior metallic interconnects vis a vis Au or Pt nano wires, or as a replacement for semiconductor based transistor elements in nano electronics[1-12]. Key factors that influence the current carrying capacity of the CNT as an interconnect are both *intrinsic* and *geometry* related. The *intrinsic* factors include the diameter (D) and length (L) of the CNT and the quality of its graphitic shells, degree of crystillanity and presence of defects etc. The *geometry* related factors include the design or the *lay-out* of the nano circuit and contact resistance/area during electrical transport measurements.

I-V data on an individual CNT with simultaneous TEM imaging brings out the correlation of both *intrinsic* and *geometry* related factors with the current carrying capacity of the CNT[1-5]. For instance, it is observed that current rises with increasing voltage upto a critical value for a CNT during I-V scans in suspended geometry. One of the contributions in the non-linear rise in 'I' with increasing 'V' up to a critical value is associated with annealing of the random defects present in the graphitic shells of the CNT. This defect annealing arises from Joule heating driven temperature rise, leading to self heating of a CNT under bias[1-5]. This self heating improves the quality of the graphitic shells of CNT, resulting in reduced carrier scattering and consequently larger current. Beyond the critical voltage (at which the current reaches its peak), a drop in current is observed, which is accompanied by a progressive deformation and burning of the graphitic shells of the CNT. In this voltage range, Joule heating is detrimental, leading to the eventual breakage of CNT at another critical voltage[1-5]. These critical parameters during a typical I-V scan on an individual CNT vary with the length, diameter as well as random defects present in its graphitic shells. The current carrying capacity of a CNT not only relates to these *intrinsic factors* but also to the *geometry* related factors[1-10]. For instance, I-V characteristics on an individual CNT have been studied earlier in a suspended geometry or when it lies over a substrate[1], both of which are *geometry* related factors. These factors crucially influence the heat dissipation paths during I-V scans and consequently influence the current carrying capacity[1-10]. Thus heat dissipation mechanism or thermal heat management are important issues in nano electronics based on CNT or otherwise[1-10].

In this work we explore electron transport on individual multiwall CNT filled with Cr_2O_3 with simultaneous TEM imaging in suspended geometry and provide the first step in exploring the utility of Cr_2O_3 filled CNT in nano scale devices. We also emphasize that while a significant amount of work has also been carried out on the encapsulation of metals inside CNT[11-15], I-V characteristics have mostly been reported for Fe-filled CNT, where the focus has primarily been on deciphering the mechanism of mass transport in femtogram scales, and the utility of metal-filled CNT as a nano pippet[13-15]. Encapsulation of multifunctional oxides[16] inside CNT, especially their I-V characteristics are relatively less explored area, though oxides such as V_2O_5[17] and CrO_3[18] have earlier been encapsulated inside CNT. While encapsulation of CrO_3 inside CNT is significant for catalysis related applications[18], it is also a precursor material for the formation of two different chrome oxides, CrO_2 and Cr_2O_3, both of which are relevant for spintronic applications[19-24].

Cr_2O_3 is a room temperature antiferromagnet[20] (T_N~307K), the most stable[21] among binary chrome oxides and environmentally benign (unlike hexavalent CrO_3) and is therefore suitable for practical applications. Significantly, Cr_2O_3 is also a well-known magnetoelectric, in which the magnetism can be tuned via an electric field[22-24]. Upon nanoscaling, it is seen to develop traits of a new functionality, piezomagnetism[25] or the stress induced magnetism. In this context, it is important to recall that while bulk Cr_2O_3, which is inherently antiferromagnetic and magnetoelectric[22-25] but not piezomagnetic, can generate this trait in ultra thin film form[26]. Thus, the magnetic encapsulate within CNT[27] realises a hybrid nanomaterial in which the magnetic properties can be tuned with ***magnetic field, electric field, and possibly stress.*** These factors can be particularly relevant in the area of antiferromagnetic spintronics[28] and the electric field control of magnetism[29].

First part of our work relates to the application of *specific experimental protocols* during conventional two probe I-V scans, which result in controlled Joule heating and a sequential restructuring of the oxide encapsulate. In this context, it is important to note that degradation of oxides during device patterning has been a major bottleneck in oxide electronics[16]. Our work brings into fore the usage of filled CNT as a nano furnace, by proper utilization of self heating. This enables *in-situ* formation of various morphological phases of a multi -functional oxide that can remain preserved inside the CNT. Further, we demonstrate that the presence of the insulating encapsulate within the CNT is linked to better heat dissipation and therefore enhanced current flowing through the CNT. Finally we also report bulk magnetization measurements on CNT elucidating the unusual magnetic properties of the encapsulate which is preserved inside the CNT.

2. Experimental

The Cr_2O_3 filling inside CNT is achieved by a two-step post-synthesis filling procedure and is characterized by analytical TEM[27]. The pristine multiwall CNT used for the filling purpose were synthesized by Chemical Vapour Deposition. Filling procedure involving capillary action was achieved using (i) pristine CNT (ii) pristine CNT, further subjected to high temperature annealing[30] (***Supp. Info: Text S1).*** In both these cases, Cr_2O_3, in the form of polycrystalline wires, was seen to fill the core cavity of the CNT. The outer diameter of such oxide - filled CNT are in the range of 20 nm to 75 nm and lengths upto 5µm. A representative TEM image for a typical (filled) multiwalled CNT is shown in **Figure**

1a. Here, the encapsulate in the form of a scanty nano wire is visible within the core cavity of the CNT. It is to be noted that in these samples, Cr_2O_3 is also seen to fill the space between the graphitic shells of the CNT. This filling can also be seen as a line guided by an arrow, alongside the filling within the core cavity of the CNT in **Figure 1a.** Though our synthesis procedure does not allow a control over this frequently seen trapping of the encapsulate *in-between* the graphitic shells, this has been unambiguously identified to be Cr_2O_3 with clear chromium and oxygen peaks through Electron Energy Loss Spectroscopy (EELS) in TEM in a large number of filled CNT. These EELS results are reported in an earlier publication[27].

The I-V measurements on the individual multiwall CNT (both filled and pristine) reported in this work are carried out using *in-situ* TEM / Scanning Tunnelling Microscopy (STM) Nanofactory holder in both JEOL 2010 (operated at 200 kV) and JEOL 3000f. Magnetization measurements are conducted using Superconducting Quantum Interface Device (SQUID) from Quantum Design.

3. Results & Discussion

3.1: I-V scans with in-situ TEM imaging : Schematic and experimental protocol

For the I-V studies, the CNT is suspended between two Au electrodes, across which a dc electrical voltage is applied and the resulting current is measured. The schematic of two probe |I-V measurements with simultaneous TEM imaging is shown in **Figure 1b**. In this schematic, a TEM image of a typical pristine CNT, hanging in suspended geometry is shown. The voltage is applied in two experimental protocols: (i)'Slow Scan' in which a fixed dc voltage is applied and held for a few tens of seconds. This process is repeated at regular intervals (~few tens of seconds) for different voltages. For a typical *slow* scan, ranging from 0.5V to 3V, step ΔV can be ~ 0.2 - 0.5V (ii) 'Fast Scan', in which the dc voltage is progressively ramped from 0 up to $\pm V_{max}$ with well-defined bias steps ($\Delta V \sim 2mV$). Here, each voltage pulse (0 upto $\pm V_{max}$) is ramped for a very short time, of the order of a few milliseconds. The crucial difference between the *slow* and the *fast* scan is holding time of the bias voltage. This can be of the order of few tens of seconds for a typical *slow scan* and a few milliseconds for a typical fast scan. Typical resistance value of the multiwall CNT, both filled and pristine used in this work ranges from a few kΩ to a few tens of kΩ. In each I-V scan, following either *slow* or *fast* scan, care has been taken to first stabilize the contact resistance before applying larger bias voltages that can result in any morphological phase changes of the encapsulate. (***supp. Info: Text S2)***.

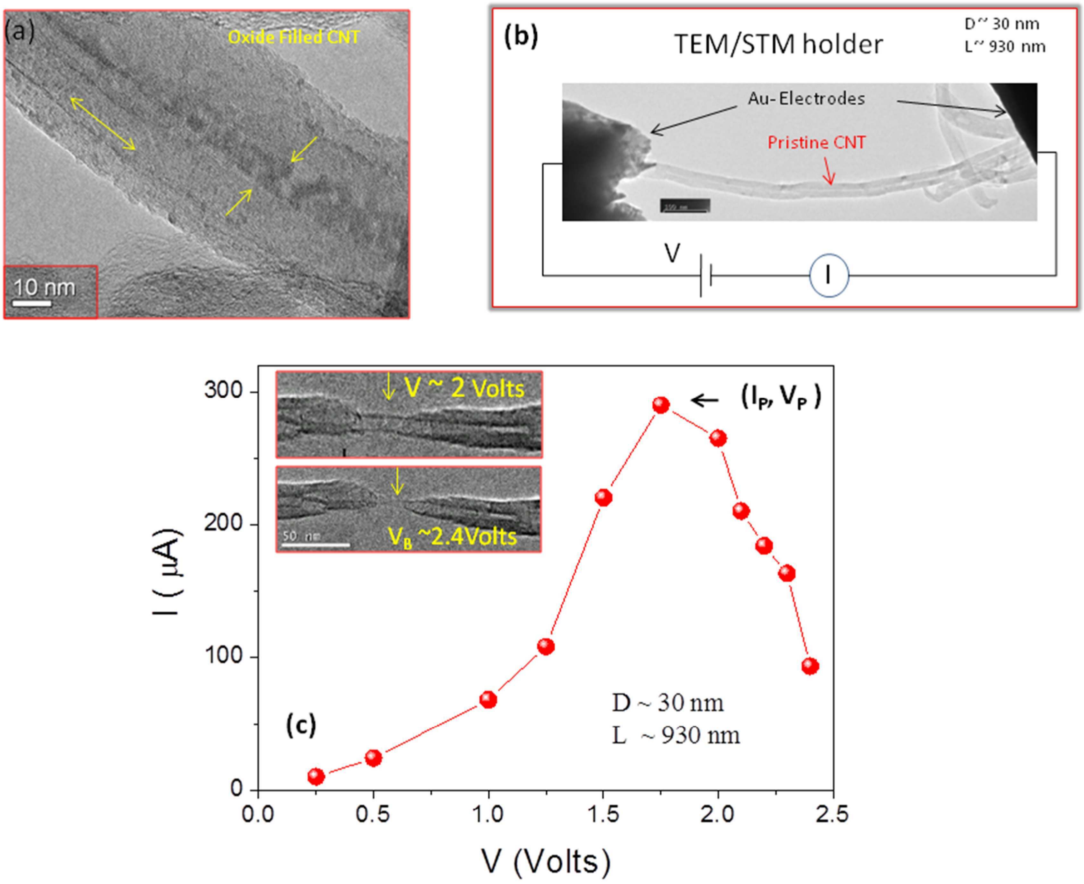

***Figure 1**: **(a)** TEM image of a typical filled CNT, depicting the oxide encapsulate within its core and in- between its graphitic shells. Arrows are the guide to the eye. **(b)** Real time image of a pristine CNT in suspended geometry, along with the schematic of two probe |I-V measurements with simultaneous TEM imaging. **(c)** I-V data following a slow scan protocol on the same pristine CNT show in the upper schematic**. Upper TEM image depicts damaged walls of the CNT observed at the bias voltage ~2 V . Lower TEM image is recorded at V_B ~2.4 volts, at which CNT is seen to break.*

Figure 1c shows an I-V scan, following a *slow* scan protocol on a pristine CNT with D ~ 40 nm; L ~ 930 nm, having resistivity ~ 10^{-5} Ω-m. This is the same pristine CNT for which TEM image is shown in **Figure 1b.** During I-V scan, current first rises with increasing voltage and reaches a peak value "I_P" at a critical voltage "V_P". For the CNT shown in **Figure 1b**, V_P ~ 1.7 Volts and I_P ~ 290 µA. On increasing the bias voltage beyond V_P, the current is seen to drop which is accompanied by a visible deformation of its graphitic shells. A TEM image of a segment of this CNT in the upper inset of **Figure 1c,** depicts the deformed graphitic shells and broken walls at the bias voltage V ~ 2 Volts. On approaching another critical voltage referred to as V_B (~ 2.4 Volts in this case) the CNT is seen to break, as shown in the lower TEM image in **Figure 1c.** These results are in qualitative agreement with earlier reports[1-5] manifesting the effects of Joule heating driven temperature rise.

In case of a metal filled CNT, such as Fe filled CNT reported in literature[13-15], the Joule heating driven temperature rise influences the graphitic shells of the CNT as well as the metallic encapsulate, which is seen to melt and move during I-V scans[13-15]. In the following we demonstrate that in case of oxide filled CNT, by variations in the amplitude and holding time of the bias voltage, the encapsulate can be converted to a desired morphology.

3.2 : Restructuring of the encapsulate during I-V Scans

Figure 2a-2d show segments of a typical Cr_2O_3-filled CNT under bias, following the *slow scan* protocol during I-V scan. A sequential restructuring of the encapsulate, from the initial state of a scanty nano wire to well separated beads and crystals, is observed in real time when the voltage was varied from 500 mV to 1800 mV, in the steps ~ 200 mV. The current is also measured as a function of time for each voltage step as shown in **Figure 2e**. The step like features in I vs Time graph are associated with amplitude changes of the applied voltage, as indicated in **Figure 2e**. The total time span is about 5 minutes for the entire I-V scan. However, for the sake of clarity, only a few representative voltages are marked in

Figure 2e. At each voltage step, the holding time is of the order of a few tens of seconds. The exact holding time is also evident from **Figure 2e**. It is to be noted that for higher amplitude of the bias voltage, current rises steadily for a fix value of V. This is seen to occur when the encapsulate melts and converts into beads or crystal. On the contrary, the current as a function of time remains rather constant at lower amplitude of the bias voltage, when there is no restructuring of the encapsulate. These features are guided by red arrows in **Figure 2e**. A clip from the video (**Supp. Info : Video S1 clip**) in the time period between 120 - 180 seconds shows the encapsulate in the form of continuous filling converting into well separated beads. Full video covering entire I-V scan (~5 minutes), can be seen in **Supp. Info : Video S1 full**) .

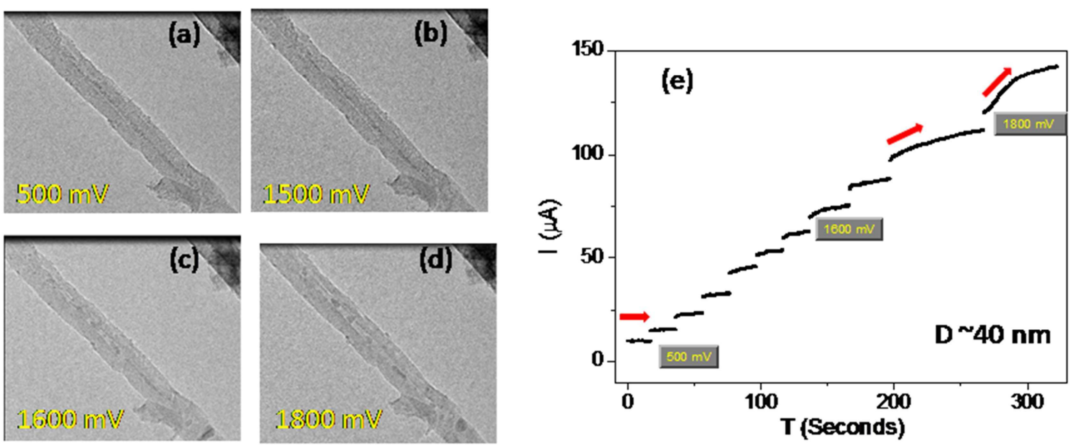

Figures 2(: (a)-(d) *are TEM snap shots for a typical Cr_2O_3 filled CNT during I-V scans, following the slow scan protocol described in text. The encapsulate remains in the form of a nano wire within the core cavity for V ~ 1 V. Well separated beads and crystals are observed with progressively increasing bias voltages.* ***(e)*** *Current vs. Time data for various bias voltages.*

Similar experiments conducted on more than a dozen oxide–filled CNT with varying diameters and lengths and filling fractions reveal that it is possible to restructure the encapsulate with discrete dc voltage pulses, roughly between 1 -3 volts. This restructuring is observed while measuring I-V in both *slow* and *fast* scans. The nano-crystals formed during

I-V scans can be preserved by removing the bias (**Figure 3a -3b)**. We also observe that depending on the initial amount of the encapsulate as well as its location over the length of the CNT, fairly big crystals can be formed. Such big crystals are more frequently seen near the contact end (the Au electrodes) where encapsulate tends to collect in the molten form **(Supp. Info : Vid. S2).** We also observed that formation of big crystal can deform the graphitic shells of the CNT. One such crystal with its clear facets formed within a CNT under prolonged bias has been shown in **Figure 3(b).**

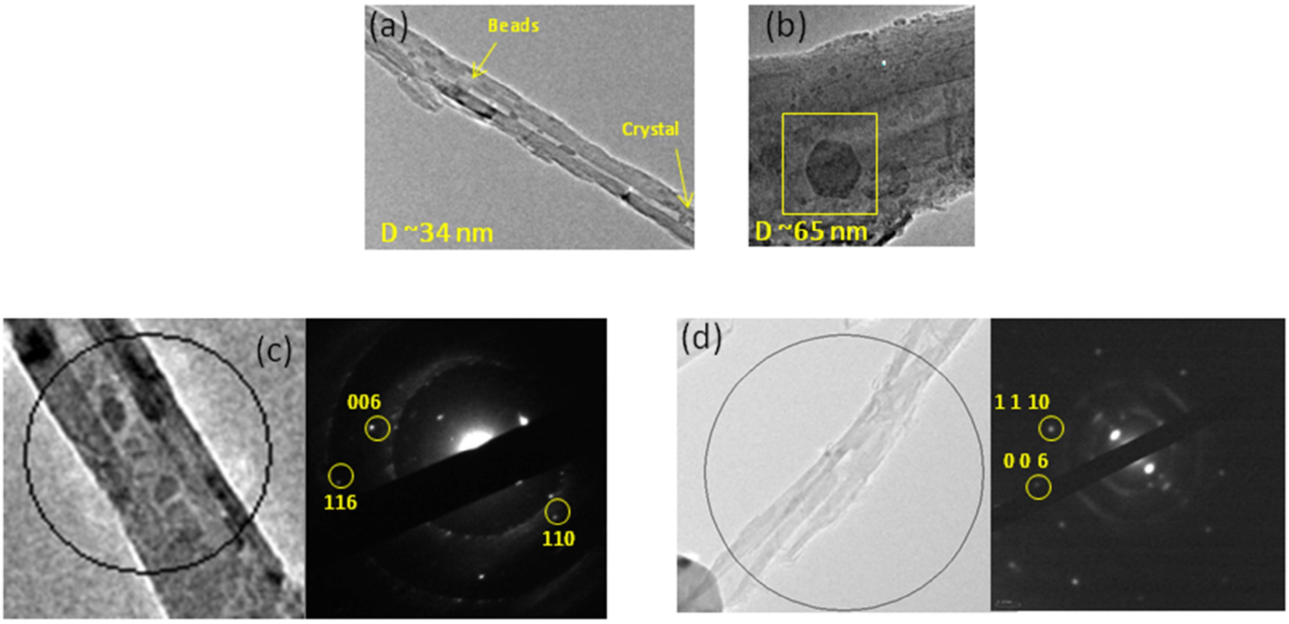

Figure 3: ***(a)*** *Formation of beads and crystals at different locations within the core cavity of self heated CNT.* ***(b)*** *Hexagonal shape Cr_2O_3 particle with clear facets formed near the contact end during I-V scan. Right panel in* ***(c)*** *shows electron diffraction on encircled area in CNT, confirming presence of Cr_2O_3 in the form of beads and crystals. The encircled area in* ***(d)*** *shows* segment of a *CNT in which the oxide encapsulate has either been flown out at the contact end or evaporated during I-V scans. However, the ED on the right panel of (d) confirms the presence of Cr_2O_3 in the form of thin sheets.*

3.3 : Characterization of individual morphological phases of the encapsulate

Once a particular phase is well formed during a I-V scan and preserved by removing the bias voltage, Electron Diffraction (ED) can be recorded on a thermally stabilized CNT under zero bias. A representative is shown in **Figure 3c**, confirming the presence of Cr_2O_3 in the form of beads and crystals. We also emphasize that we could not find any evidence of elemental chromium in ED data obtained on a number of CNT, thus ruling out the possibility of reduction of Cr_2O_3 to elemental chromium. Another important observation is that on reversing the polarity of voltage during I-V scans, the oxide beads or crystals do not move in opposite direction. This is different from the case of Fe filled CNT where the metallic encapsulate is seen to move in the reverse direction on reversing the polarity during I-V scans[13-15].

The nano crystals formed within CNT under bias can also be re-melted on further increasing the bias voltage. This melt is seen to flow within the core-cavity and also it can flow out at the contact end (**supp. Info Videos S2-S4).** While the encapsulate evaporating or flowing out of the CNT is a common observation[13-15], we find that by controlled variations in V, the oxide visibly shows a tendency to flow *in-between* the graphitic shells of CNT ***(Supp. info : Text S3)***. A tendency for the encapsulate to exist *in-between* the graphitic shells was observed during routine TEM characterization of these oxide filled CNT[27]. However, real time observation of this phenomenon during I-V scans further confirms that for Cr_2O_3 in molten form, the surface tension conditions are conducive for it to flow in sub nanometer scale.

For confirming the presence of Cr_2O_3 is sheet stage, the amplitude of the voltage was increased such that the nano crystals and beads formed within the CNT either flow out from the contact end, or evaporate. To obtain this state, V is intentionally increased well above V_P to ensure that no crystals or beads are seen across the length of the CNT and a seemingly empty CNT is left. A representative is shown in the left panel. The ED patterns recorded on the enclosed segment of the CNT is shown in the right panel of **Figure 3d.** This confirms the presence of the chrome oxide in the form of ultra thin sheets within CNT. (**Supp. Info : Figure S1** & **Video S4)**

Here it is important to note that due to the resolution issues in TEM imaging *while* performing electrical transport measurements, the encapsulate in the form of thin oxide sheets cannot be as clearly imaged as for the situation in which it is in the form of beads or nano crystals within the CNT. It is also important to image a broad segment of the CNT during I-V scans, in order to track the morphology of the encapsulate across its length. However for seemingly empty tube under both slow or fast scan, ED shows presence of chrome oxides.

The possibility to form a thin oxide sheet in a controlled manner during I-V scans is a particularly interesting observation. Since Cr_2O_3 is not a typical 2-dimensional material that can be easily exfoliated into sheets similar to graphene or MoS_2, the controlled variation of V with proper utilization of self heating can be a route to form and preserve ultra thin sheets of Cr_2O_3 and possibly other functional materials inside CNT. This can be particularly relevant for exploring interface effects in oxides[31].

Snapshots presented in Figure 2 and 3 confirm that the filled CNT in suspended geometry, under controlled bias can act as a nano-furnace, in which beads, nano-crystals or sheets of Cr_2O_3 can be ***fabricated*** and ***preserved.*** The generic nature of this behaviour points towards the possibility of achieving the same in other functional materials. For instance, a filled CNT can easily be patterned to lie over a trench in suspended geometry, similar to what was achieved for pristine CNT by Pop et.al[1] and the functional magnetic oxide can be reshaped/ restructured by controlled voltage modulations, as shown here. This can have significant implications in on-spot formation of desired phase/ morphology, as oxides are known to exhibit deterioration in their functional properties during device fabrication procedure[16].

From the I-V data collected over a large number of filled CNT, we find some interesting correlations between current flowing in the CNT and various morphological phases of the encapsulate. We observe that for a given voltage, the current flowing in the CNT is systematically larger when the encapsulate is in the form of beads or crystals as compared to the case when it is in the form of a scanty nano wire. The rise in current, when the encapsulate is in different morphological phases, is observed in both experimental protocols, the *slow* and the *fast* I-V scans.

3.4 : Restructuring of the encapsulate and current enhancement

We first discuss current enhancement in various stages of the encapsulate prepared and preserved following a *slow* scan protocol. For these measurements, I-V scans limited to ±1 Volt is recorded at the initial stage, when the oxide is in the form of nano wire. Thereafter the encapsulate is intentionally converted to beads (or crystals) using a *slow scan* protocol and this phase is preserved by switching off the bias. Waiting for a sufficiently long time (after switching off the bias) enables thermal stabilization of the CNT. Thereafter, I-V scan, limited upto ±1 Volt' is again recorded. The reason to limit the bias voltage upto ±1V is that voltages of this magnitude do not further change the existing morphological phase. Such limited scans, recorded at different states of the encapsulate are shown in **Figure 4a,** depicting that the current for a given voltage is systematically higher when the encapsulate is in the form of beads and crystals.

To explore the correlation between restructuring of the encapsulate and enhancement in the current, we further investigated the effect of faster heating time scales and recorded I-V scans *while* the encapsulate changes morphology. This was achieved following the *fast* *scan protocol* in which voltage pulse of the type (0 upto $\pm V_{max}$) are ramped for a very short time (**Figure 4b**). Here each voltage cycle (say +2 to -2 volts indicated in purple color in **Figure 4b)** is ramped within a few millseconds, which is essentially the holding time of the bias voltage during each ramp. This results in correspondingly shorter Joule heating times. In these *fast scans*, for voltage pulse in which V_{max} > 1 volt, the encapsulate changes its morphology, similar to what one also observes in a typical slow scan. *Fast* scans lead to a different pattern of formation of beads and nanocrystals as compared to patterns seen in slow scans. However, all the core observations including a systematic enhancement in the current remain the same **(Figure 4b** & **Supp. Info: Figure S2)**.

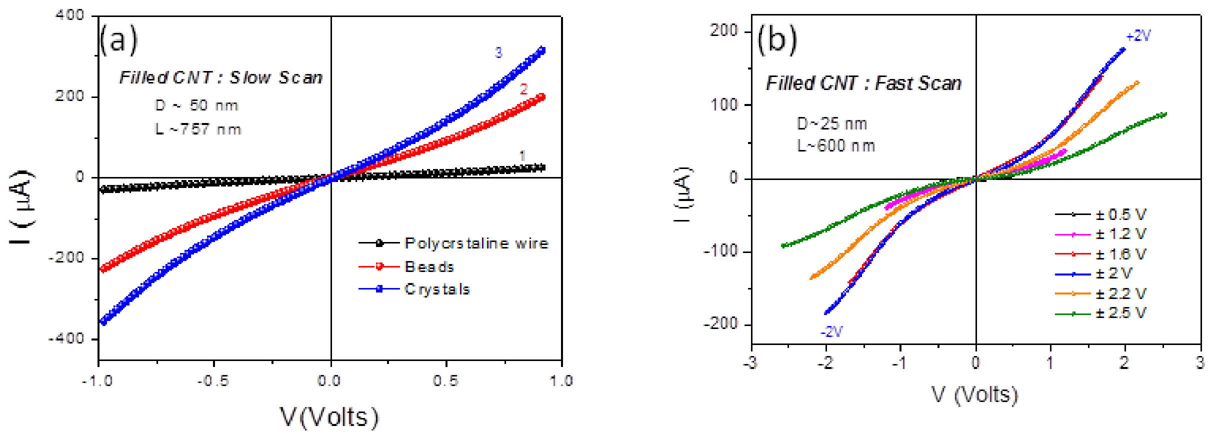

Figure 4 : I-V scan recorded using different protocols (a) *I vs V limited upto ±1 Volts, at different stages of the encapsulate. These stages have been prepared following a slow scan protocol* ***(b)*** *I-V scans, following fast scan protocol for shorter heating times, covering* $\pm V_{max}$ *within a few milliseconds.*

Overall, data in **Figure 2e** and **Figure 4** indicate that there is an enhancement in the current when systematic restructuring of the encapsulate takes place. However, from the statistics collected over a large number of CNT, we find that the magnitude of this current enhancement can be different for CNT with varying diameters lengths and filling fractions.

In order to investigate the possible reasons for the observation of current enhancement in filled CNT, We first compare the I-V scans in pristine CNT and filled CNT so as to isolate the possible role of the encapsulate, particularly when it restructures. We take into account both *intrinsic* factors (related to the dimension/defect density in the graphitic shells of the individual CNT) as well as the *geometry* related factors (related to the layout of the nano circuit) so as to understand the possible reason of current enhancement.

3.5 : I-V scans : Pristine vis a vis filled CNT

We first recall the I-V characteristics investigated in the past for CNT[1-7]. Here a key result is that as a function of applied voltage, current is higher for the CNT with larger diameter and shorter length[4]. In addition, each graphitic shell can have random defects, which also influences the current flowing in the CNT. These random defects can get annealed out during I-V scans when Joule heating driven temperature rise is sufficient. Such random effects associated with the graphitic shells are likely to be present in both pristine and the filled CNT. Annealing of such defects can give rise to reduced carrier scattering and slightly enhanced current in both cases. Thus value of V_P and I_p is likely to vary with the length, diameter and defect density[1-5] corresponding to each CNT; filled or pristine.

Apart from the above mentioned factors, a key difference between filled and pristine CNT is that each filled CNT may have different extent of filling in its *as-prepared* stage. In addition, contact resistance/ area can also vary significantly for each I-V scan. Thus it is non-trivial to isolate the various contributions related to dimension factor, defect density and amount of filling and quantify the enhancement in current, particularly while measuring two probe I-V scans with simultaneous TEM imaging. It is also practically difficult to locate a pristine and a filled CNT of similar dimensions.

However, we compare I-V scans of one pristine (red dots) and one filled (blue dots) of approximately similar diameter in **Figure 5a**. Both I-V scans are recorded under *slow scan* protocol. Here a normalized quantity I/I_{500mV} is plotted against the bias voltage V for each CNT. This normalization in current enables us to get rid of variations in dimensions as well as the contact resistance. Here I_{500mV} ('I' measured at applied bias V~500 mV) for normalization was chosen for two reasons. (i) For voltage scans upto 500 mV, the contact resistance is unhysteretic and reproducible over multiple scans. (ii) voltage scans upto 500 mV do not lead to any significant self heating that can lead to morphological phase changes in the encapsulate. These factors are crucial for a meaningful comparison of current enhancement in filled and the pristine CNT. The ***maximum*** value of the normalized current in $I/I_{500\ mV}$ vs V graph is "$I_p/I_{500\ mV}$". This value is indicative of the "current enhancement factor" for individual CNT in ***any*** I-V scan on a CNT, irrespective of its dimensions and contact resistance value. These values are highlighted by arrows for both CNT in **Figure 5(a)**.

As evident from the **Figure 5a,** both filled and pristine CNT exhibit a peak like structure in I-V pattern, which is expected for a CNT under bias in suspended geometry[1]. However, the value of $I_p/I_{500\ mV}$ is about 55 for the filled CNT and 20 for the pristine one. This data again shows a substantial enhancement in the current for the filled CNT, which is approximately three times the length of pristine CNT and also slightly less in diameter. It is also to be noted that longer CNT in hanging geometry are seen to display lower threshold value $V_{p,}$ at which maximum current I_P is reached. However, in this case we find that the filled CNT also exhibits approximately similar V_p.

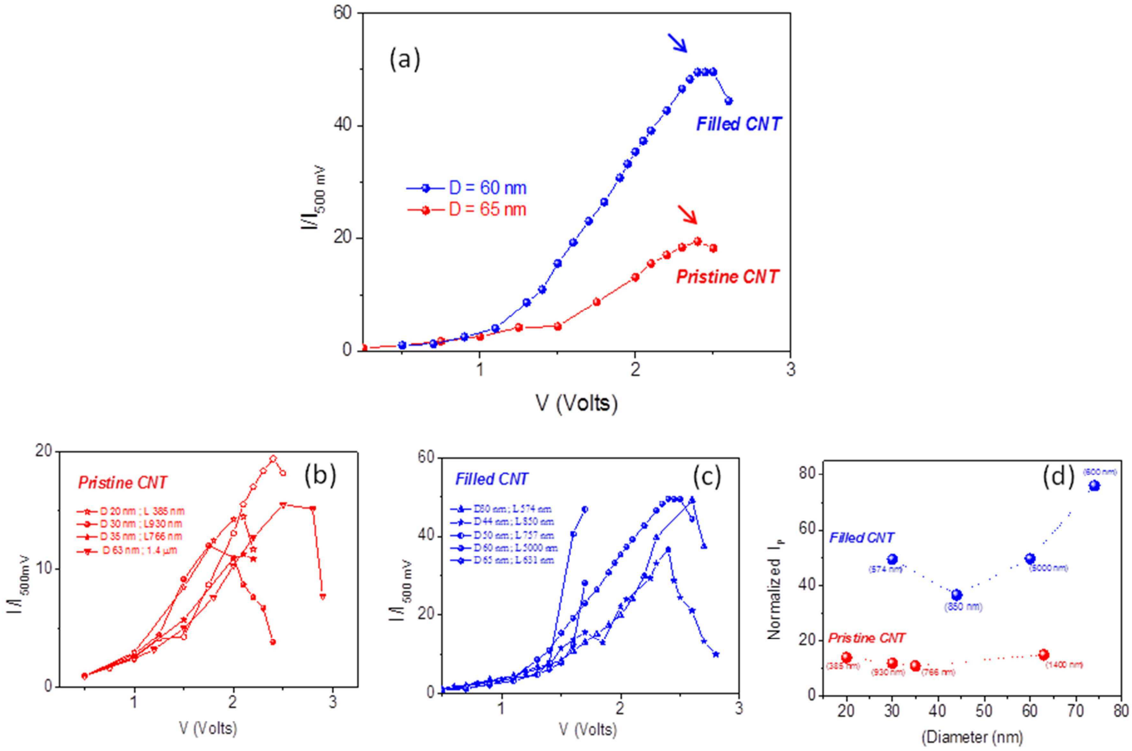

***Figure 5**: **Current Enhancement Factor of filled CNT : (a)** Comparison of the normalized current ($I/I_{500\ mV}$) as a function of bias voltage(V) for a filled CNT and a pristine CNT. The maximum value of normalized current (I_p / $I_{500\ mV}$) in filled CNT is about three times in magnitude as compared to the pristine one. Normalized I-V scans for a number pristine and filled CNT are shown in **(b)** and **(c)**. Normalized I_P as a function of diameter is shown in **(d)** for a number of filled and pristine CNT . The length of the individual CNT in each case is also indicated in beside each data point. Data shown in **(d)** further confirms that the average value of normalized I_P for the filled CNT is significantly large irrespective of length and diameter.*

I-V data on a number of pristine and filled CNT of various diameter and length is shown in **Figure 5b & 5c** respectively. We observe that for pristine CNT, the rise in normalized current starts to occur ~ 1 Volt. The slope at which current rises as well as the value I_p and V_p vary, depending on the dimension of individual CNT as well as defect density associated with the graphitic shells. For filled CNT, the rise starts to occur at a relatively higher value ~ 1.5 Volt, which also coincides with the restructuring of the encapsulate as observed during *in-situ* TEM imaging. As evident from the **Figure 5c**, current rises at much faster rate and normalized I_p is significantly larger. For some filled CNT, the voltage was not scanned beyond V_P so as to preserve the crystal or the beads for recording ED pattern. However the trend in the rise of the current indicates even superior current enhancement factor (blue diamonds in **Figure 5c**).

Normalized I_P (or the current enhancement factor) obtained from individual I-V scans in each case, as a function of diameter is shown in **Figure 5d** . It falls within a certain range (10-20) in case of pristine and between 40-80 in case of filled ones. These data confirms that the average value of maximum current flowing in the filled CNT significantly larger irrespective of dimensions and defect density factor. It is to be noted that all the data shown in **Figure 5**, (for comparing the current enhancement factors) are recorded following identical experimental protocol of *slow* I-V scans. Qualitatively similar results were observed during *fast scans* (not shown here) as well.

As is evident from **Figure 5**, large enhancement in current observed in filled CNT cannot be explained *only* within the framework of variations in the dimension of the CNT or the presence of the random defects in its graphitic shells. ***(Supp. Info : Text S4)*** The range of current rise due to annealing of random defects associated with the graphitic shells can be also judged from **Figure 5d**. The data contained in **Figure 5(a-d)** brings out that defect annealing of the graphitic shells exists in both pristine and the filled CNT, as both exhibit a sharper rise in normalized current, roughly above 1Volt, where Joule heating becomes significant. However current rises at much faster rate for the filled CNT and the normalized I_P is also much larger in magnitude. .

Regarding the enhancement of the current, another possibility is that of current flowing through the encapsulate, apart from the graphitic shells of the CNT during I-V scans. However, here a nano scale insulator is encapsulated within a metallic multiwall CNT. For a metallic encapsulate, such as the case of Fe filled CNT[13], possibility of current flowing through the metallic Fe core can be taken into account. However, considering the insulating nature of the encapsulate, (and for the geometry such as shown in **Figure 1b** during I-V scans) it is reasonable to assume that the current primarily flows through the graphitic shells of the CNT. ***(Supp. Info S5)***

Thus the situation in our case is that of a nano scale insulating oxide inside a metallic CNT and during I-V scans we observe a significant enhancement in current flowing through the filled CNT vis-a-vis pristine CNT. This enhancement does not seem to arise from only the dimension factor or defect density associated with a particular CNT. In the following section, we discuss a possible scenario related to the heat sinking mechanism in our filled CNT that can lead to the observed current enhancement.

3.6 : Pristine vis a vis filled CNT in suspended geometry : Heat sinking mechanism

Considering the *lay out* of the nano circuit during I-V scans, (which is a *geometry* related factor) we recall that the current flowing in a suspended CNT is slightly smaller in comparison to the case when the same is lying on the substrate[1]. Here the suspended CNT is seen to exhibit a peak like structure in I-V scans whereas the one lying on the substrate shows a saturating behaviour[1]. These features are understood to arise from better heat sinking mechanism due to the presence of the substrate[1]. It is also observed that a pristine CNT in suspended geometry during I-V scans usually breaks from the middle on approaching V_B, as the Joule heating driven temperature rise is maximum at this location[2-3]. At the contact ends, the metallic electrode provide better heat sinking mechanism. From I-V scans upto V_B on a number of filled CNT, we observe that unlike pristine CNT, the filled ones do not usually break from middle on approaching V_B. These features indicate that the heat dissipation mechanism of filled CNT in our case, though still in suspended geometry, needs to be investigated.

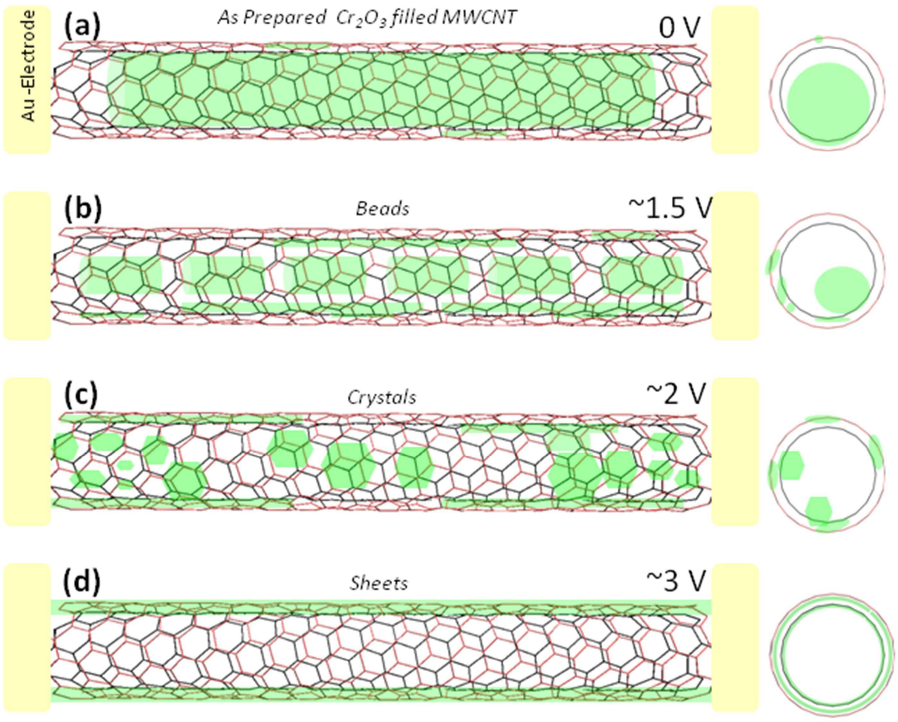

Figure 6 (a)-(d) *Schematic of Cr_2O_3 filled CNT (side and top view) depicting various morphological phases of the encapsulate being formed under progressively increasing bias*

We first note that in our case, the electrically insulating encapsulate is in thermal contact with the graphitic shells of the CNT. The filled CNT is shown schematically in **Figure 6a** where the encapsulate (green) is in the form of scanty polycrystalline nano-wire within the core cavity, with an occasional trapping in-between the graphitic shells. This depiction is for *as-prepared* filled CNT under zero bias. **Figures 6b-6d** display the effect of systematically increasing bias voltage and associated temperature rise due to Joule heating. Here the encapsulate, (through its thermal contact with the self heated CNT) melts and expands within the core cavity as is clearly observed in simultaneous *real time* TEM imaging This is followed by the systematic formation of beads and nano crystals. (**Figures 1-2, Video S1-S4**). This procedure is likely to create a more uniform coating of the encapsulate within the core cavity of the CNT, leading to a better thermal contact with the graphitic shells. On increasing the applied bias further, the nano-crystals, thus formed, re-melt and further expand, resulting in the common observation of more and more material flowing out of the CNT at the contact ends until there is no visible particle observed within the core cavity. However, a thin layer remains within the core cavity and *in –between* the graphitic shells **(Figure 3c -3d)**. Since the graphitic shells are in thermal contact with the heat sink (the Au-electrodes) the uniform coating of the oxide encapsulate is likely to provide additional / better heat sinking mechanism than what exists for a pristine CNT. This heat sinking to the Au –electrodes can be direct or through the graphitic shells of CNT.

Thus I-V scans on filled CNT indicate that various forms of the insulating filling (wire- beads-crystals -sheets) are likely to act as the heat sinks of varying capacity, providing additional heat dissipation routes along the length of the CNT and contribute in larger current flow for a given voltage, as we observe. This is also corroborated by I vs Time of **Figure 2e,** clearly exhibiting a steeper rise in current when a morphological phase changes take place in the filling. The magnitude of this substantially enhanced current in the case of filled CNT also indicates that it would be interesting to investigate the thermal conductivity[32] of each morphological phase and its contribution in the current carrying capacity of the CNT.

3.7 : Magnetic characterization of Cr_2O_3 filled CNT

Having established that *on–spot* morphological phase changes are possible for this functional magnetic oxide using CNT in suspended geometry observation of associated current enhancement, we have also explored the magnetic properties of *as–prepared* filled CNT using SQUID magnetometer. **Figure 7** shows the magnetic characterization of Cr_2O_3 is in the form of nanowires within CNT. Here, bulk magnetization (M) is measured as a function of magnetic field (H) and temperature (T). **Figure 7a** shows the M-H isotherm recorded at 10 K depicting a non-saturating behaviour of M upto the field of the order of 5 Tesla, indicative of AFM interactions. This also confirms that our sample does not contain ferromagnetic catalyst particles, which generally adhere to CNT during the routine synthesis, using Chemical Vapour Deposition[30] (**Supp. Info: Text S6**). The M vs T data measured from 310 K down to 5K in the field cooled (FC) state, is seen to increase with decreasing temperature, as shown in **Figure 7b**. This behaviour is qualitatively similar to what is seen in nanoscale antiferromagnets in general, and in nanoparticles and nanowires of Cr_2O_3[33-35].

Earlier studies have indicated that in ultra thin film form, when Cr_2O_3 appears as a surface layer in a composite system, comprising of a ferromagnetic core (CrO_2) and antiferromagnetic shell (Cr_2O_3), its magnetoelectric properties are enhanced near the room temperature[24]. In addition, it also develops traits of piezomagnetism[25] or stress induced magnetism, when appears as ultra thin surface layer in this composite[26]. We investigated if some of these traits, especially signatures of stress induced moments, are still present when Cr_2O_3 is confined within CNT. These features are explored through Thermo-Remanent Magnetization (TRM) measurements.

It is interesting to recall that the magnetization dynamics of nano scale antiferromagnets is a heavily debated topic in literature[33]. For such systems, measuring The TRM measurements (as a function of time 't' or temperature 'T') can reveal subtle magnetic features, which are not clearly visible in routine *in-field* magnetization measurements[33,35]. In addition, the TRM, which basically represents the magnetization relaxation dynamics, after the removal of the applied magnetic field, carries a wealth of information about the associated magnetic phase[26,35]. This can be crucial for nano scale antiferromagnets which have large number of uncompensated surface spin, leading to a variety of magnetic phases.

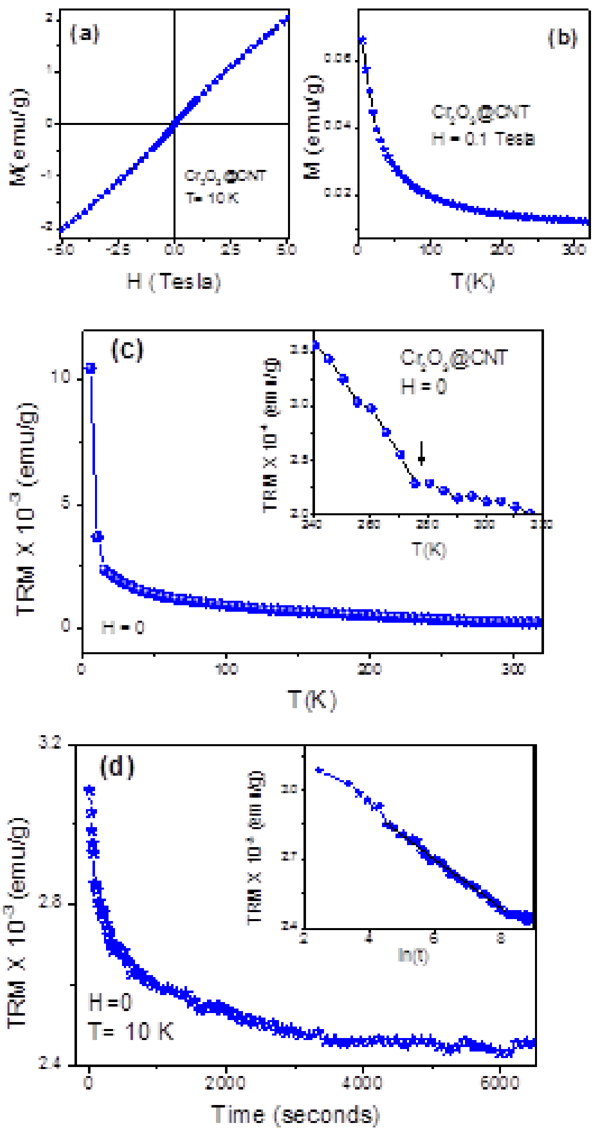

Figure 7: ***Magnetic characterization of as-prepared CNT:*** *(a) shows MH isotherm at 10K, exhibiting non saturating magnetization up to 5 Tesla. This also confirms the absence of ferromagnetic catalyst impurities in our sample.**(b)**Magnetization as a function of temperature at H = 0.1 Tesla.**(c)** Main panel shows TRM as a function of temperature, indicative of robust pinning mechanism leading to a fairly constant TRM value in a wide temperature range. The inset shows a*

change of slope around 280K, which is not clearly visible in routine or in-field M vs T measurements. ***(d)*** *shows the TRM as a function of time, exhibiting slow relaxation phenomenon, following a logarithimic dependence (inset).*

In **Figures 7c & 7d,** the TRM data is presented which has been obtained with the following protocol. First the sample is cooled in the presence of magnetic field, referred to as H_{cool} from 310 K down to 10 K. At 10 K, the magnetic field is removed and the TRM is measured in ***zero magnetic field*** either (i) as a function of increasing temperature T, from 10 K to 300 K, or **(**ii**)** as a function of time 't' up to a couple of hours.

Figure 7c shows TRM as a function of temperature showing a finite value over a wide temperature range right up to the room temperature. This indicates a magnetization pinning mechanism which is fairly robust in nature. The inset shows the same in the expanded region, between 240-320 K exhibiting a subtle change of slope around 280K. This feature in the TRM data is not as clearly seen in routine (*in –field*) M vs T data. These data also brings out the utility of TRM measurements in the cases of nano scale AFMs. It is interesting to recall that a similar feature in M vs T in isostructural compound α-Fe_2O_3 is associated with the onset of piezomagnetism or stress induced moments[36]. While bulk Cr_2O_3 does not exhibit this feature, in ultra thin film form, it has shown the possibility of piezomagnetic moments due to strain effects arising from lattice mismatch[26]. Observation of substantial TRM along with a change of slope in TRM vs T around 280 K indicates the possibility of stress induced moments when Cr_2O_3 is confined within CNT in the form of *nano -wires* .

Figure 7d shows TRM as a function of time, measured over a time period of about 1.5 hours, exhibiting slow relaxation phenomenon. The inset shows that the magnetic relaxation or the time dependence of the TRM is logarithmic in nature. This is different from exponential decay, seen in Fe filled CNT[37], indicating unusual magnetic properties of the oxide encapsulate within CNT. These data further confirm unusual magnetic state of Cr_2O_3, particularly through the observation of a long lived remanance[26], which can be associated with the onset of stress induced moments in this system.

More importantly, the functional magnetic properties exist near the room temperature where nano spintronic devices are expected to work. It is also evident that its magnetic properties, when it systematically forms as beads, nano crystals and sheets inside an individual CNT will be interesting from both theoretical and experimental point of view. The magnetic properties on individual CNT can also be explored using the technique of micro Hall Magnetometry[38] , and such measurements are planned for the future.

4. Conclusion

In summary we show the possibility of changing the morphological phase of a multi functional magnetic oxide encapsulated and protected inside carbon nanotubes. This is achieved via modulations in amplitude, rate and holding time of the bias voltage during two probe I-V measurements on individual CNT in suspended geometry and points towards the possibility of achieving the same in other functional oxides. We further demonstrate that the presence of an insulating filling inside the CNT serves as a pathway to heat sink or acts as a substrate within the CNT, leading to the enhancement in current flowing through the CNT. This can be promising for enhancing the current carrying capability of CNT as interconnects and for better thermal heat management in nano electronics. Novel nano-spintronic devices can be envisaged, comprising of unique magnetic and electrical properties of the oxide encapsulate, which is protected inside the graphitic shells of carbon. In addition, graphitic shell of the multilwall or single wall carbon nanotubes, can provide either metallic or semiconducting contact according to a specific application for device patterning.

Supporting Information

Text S1-S6, Figures S1-S2, Video S1- S4 have been given as supporting information.

Conflict of Interests:

The authors declare no competing Financial Interests

Acknowledgements

AB acknowledges DST, India for support though a Ramanujan Grant. AB also acknowledges help from Science Media Centre of IISER Pune. Authors thank Dr. S Nair, IISER, Pune for SQUID magnetization measurements and Dr S Gorantala for HR-TEM images.

References

[1] Pop E, Mann D, Cao J, Wang Q, Goodson K, Dai H. Negative Differential Conductance and Hot Phonons in Suspended Nanotube Molecular Wires. Phy. Rev. Lett. 2005; 95: 155505-4.

[2] Huang JY, Chen S, Jo SH, Wang Z, Han DX, Chen G, Dresselhaus MS, Ren ZF. Atomic-Scale Imaging of Wall-by-Wall Breakdown and Concurrent Transport Measurements in Multiwall Carbon Nanotubes. Phys. Rev. Lett. 2005; 94: 236802-4.

[3] Kuroda M.A, Cangellaris A, Leburton J.P. Nonlinear Transport and Heat Dissipation in Metallic Carbon Nanotubes. Phys. Rev. Lett. 2005; 95: 266803-4.

[4] Bourlon B, Glattli DC, Plaçais B, Berroir JM, Miko C, Forró L, Bachtold A. Geometrical Dependence of High-Bias Current in Multiwalled Carbon Nanotubes. Phys. Rev. Lett. 2004; 92: 026804-4.

[5] Collins PG, Hersam M, Arnold M, Martel R, Avouris Ph. Current Saturation and Electrical Breakdown in Multiwalled Carbon Nanotubes. Phys. Rev. Lett. 2001; 86: 3128-4.

[6] Costa Pedro MFJ, Gautam Ujjal K, BandoY, Golberg D. Direct Imaging of Joule Heating Dynamics and Temperature Profiling inside a Carbon nanotube Interconnect. Nature Communications, 2011; 2: 1429-6.

[7] Anantram MP, F. Leonard, F. Physics of Carbon Nanotube Electronic Devices. Rep. Prog. Phys. 2006; 69: 507-561.

[8] Subramaniam C, Sekiguchi, A, Yamada T, Don N. Futaba, Kenji Hata. Planar and Multi-tiered Current Pathways from a Carbon nanotube-Copper Composite with High Conductivity, Ampacity and Stability. Nanoscale 2016; 8: 3888-3894

[9] Martel R, Schmidt T, Shea H. R, Hertel T, Avouris ph. Single- and Multi-wall Carbon Nanotube Field-Effect Transistors. Appl. Phys. Lett. 1998; 73: 2447-2449.

[10] Collins P.G, Arnold MS, Avouris P. Engineering Carbon Nanotubes and Nanotube Circuits Using Electrical Breakdown. Science, 2001; 292: 706-709.

[11] Aslam Z, Nicholls R, Koos A, Nicolosi N, Grobert N. Current-Induced Restructuring and Chemical Modification of N-Doped Multi-walled Carbon Nanotubes. Advanced Functional Materials 2011; 21: 3933-3937.

[12] Monthioux M, Filling Single-wall Carbon Nanotubes. Carbon, 2002; 40: 1809–1823.

[13] Svensson K, Olin H, Olsson E, Nanopipettes for Metal Transport. Phys. Rev. Lett. 2004; 93: 145901-4.

[14] Loeffler M, Weissker U, Muhl T, Gemming T, Eckert J, Buechner B. Current-Induced Mass Transport in Filled Multiwalled Carbon Nanotubes. Advanced Materials, 2011; 23: 541-544.

[15] Coh S, Gannett W, Zettl A, Cohen ML, Louie SG. Surface Atom Motion to Move Iron Nanocrystals through Constrictions in Carbon Nanotubes under the Action of an Electric Current. Phy. Rev. Lett. 2013; 110: 185901-5.

[16] Editorial, *Nature Materials*, 2012; 11: 91.

[17] Ajayan PM, Stephan O, Redlich PH, Colliex A. Carbon nanotubes as Removable Templates for Metal Oxide Nanocomposites and Nanostructures. Nature, 1995; 375: 564-567.

[18] Mittal J, Monthioux M, Allouche H and Stephan O. Room Temperature Filling of Single-wall Carbon Nanotubes with Chromium Oxide in Open Air, Chem. Phys. Lett. 2001; 339: 311-318.

[19] Zutic I, Fabion J, Sarma SD. Spintronics: Fundamentals and Applications. Rev. Mod. Phys.2004; 76: 323-410.

[20] Hwang HY, Cheong S.-W. Enhanced Intergrain Tunneling Magnetoresistance in Half-Metallic CrO_2 Films. Science 1997; 278: 1607-1909.

[21] Bajpai A, Nigam AK. Chromium dioxide (CrO_2) and Composites of Chromium dioxide and other Oxides of Chromium such as CrO_2/Cr_2O_3 and CrO_2/Cr_2O_5 and Process for Manufacturing the same. US patent # *7276226*.

[22] Fiebig M. Revival of the Magnetoelectric Effect. J. Phys. D: Appl. Phys. 2005; 38: R123-R152.

[23] Gehring GA. On the Microscopic Theory of the Magnetoelectric Effect. Ferroelectrics, 1994; 161: 275-285.

[24] Bajpai A, Borisov P, Gorantala S, Klingeler R, Thomas J, Gemming T, Kleemann, W, Buechner B. Interface-driven Magnetoelectric Effects in Granular CrO_2, Euro Phy. Lett. 2010; 91: 17006.

[25] Borovik-Romanov A.S. Piezomagnetism in the Antiferromagnetic Flurides of Cobalt and Manganese. Sov. Phys. JETP, 1960; 11: 786-793.

[26] Bajpai A, Klingeler R, Wizent N, Nigam AK, Cheong S.-W., Buechner B. Unusual Field Dependence of Remanent Magnetization in Granular CrO2: Possible Role of Piezomagnetism. J. Phys. Cond. Matt. 2010; 22: 096005-6.

[27] Bajpai A, Gorantla S, Loeffler M, Hampel S, Ruemmeli MH, Thomas J, Ritschel, M, Gemming T, Büchner B, Klingeler R. The Filling of Carbon Nanotubes with Magnetoelectric Cr_2O_3, Carbon, 2011; 50: 1706.

[28] Barthem VMTS, Colin CV, Mayaffre H, Julien M.-H, Givord D. Revealing the Properties of Mn_2Au for Antiferromagnetic Spintronics. Nature Communications, 2013; 4: 2892-7.

[29] Matsukura F, Tokura Y and Ohno H. Control of Magnetism by Electric Fields. Nature Nanotechnology, 2015; 10: 209–220.

[30] Lipert K, Kretzschmar F, Ritschel M, Leonhardt A, Klingeler R, Büchner B. Non Magnetic Carbon nanotubes J. Appl. Phys, 2009; 105: 063906-4.

[31] Chakhalian J, Freeland JW, Millis AJ, Panagopoulos C, Rondinelli JM. Emergent Properties in Plane View: Strong Correlations at Oxide Interfaces. Rev. of Mod. Phy. 2014; 86: 1189-1202.

[32] Choi TY, Poulikakos D, Tharian J, Sennhauser U. Measurement of the Thermal Conductivity of Individual Carbon Nanotubes by the Four-Point Three-ω Method. Nano Lett., 2006; 6:1589-4.

[33] Mørup S, Frandsen C. Thermoinduced Magnetization in Nanoparticles of Antiferromagnetic Materials Phys. Rev. Lett.2004; 92: 217201.

[34] Halley D, Najjari N, Majjad H, Joly L, Ohresser P, Scheurer F, Ulhaq-Bouillet C, Berciaud S, Doudin B, Henry Y. Size-induced enhanced magnetoelectric effect and multiferroicity in chromium oxide nanoclusters. Nature Communications, 2014; 5: 3167-9.

[35] Benitez MJ, Petracic O, Tüysüz H, Schüth F, Zabel H. Fingerprinting the Magnetic Behavior of Antiferromagnetic Nanostructures using Remanent Magnetization Curves. Phy. Rev. B, 2011; 83: 134424.

[36] Phillips TG, White RL. Piezomagnetism of α-Fe_2O_3 and the Magnetoelastic Tensor of Fe3+ in Al_2O_3. Phys. Rev. 1967; 162: 382-6.

[37] Dillon F.C, Bajpai A, Koós A, Downes S, Aslam Z, Grobert N. Tuning the Magnetic Properties of Iron Filled Carbon Nanotubes**.** Carbon, 2012; 50: 3674-7.

[38] Das P, Porrati F , Wirth S, Bajpai A , Ohno Y ,Ohno H , Huth M, Müller J. Domain wall dynamics in a single CrO_2 grain. J. Appl. Phys. 2201;112: 053921-6.

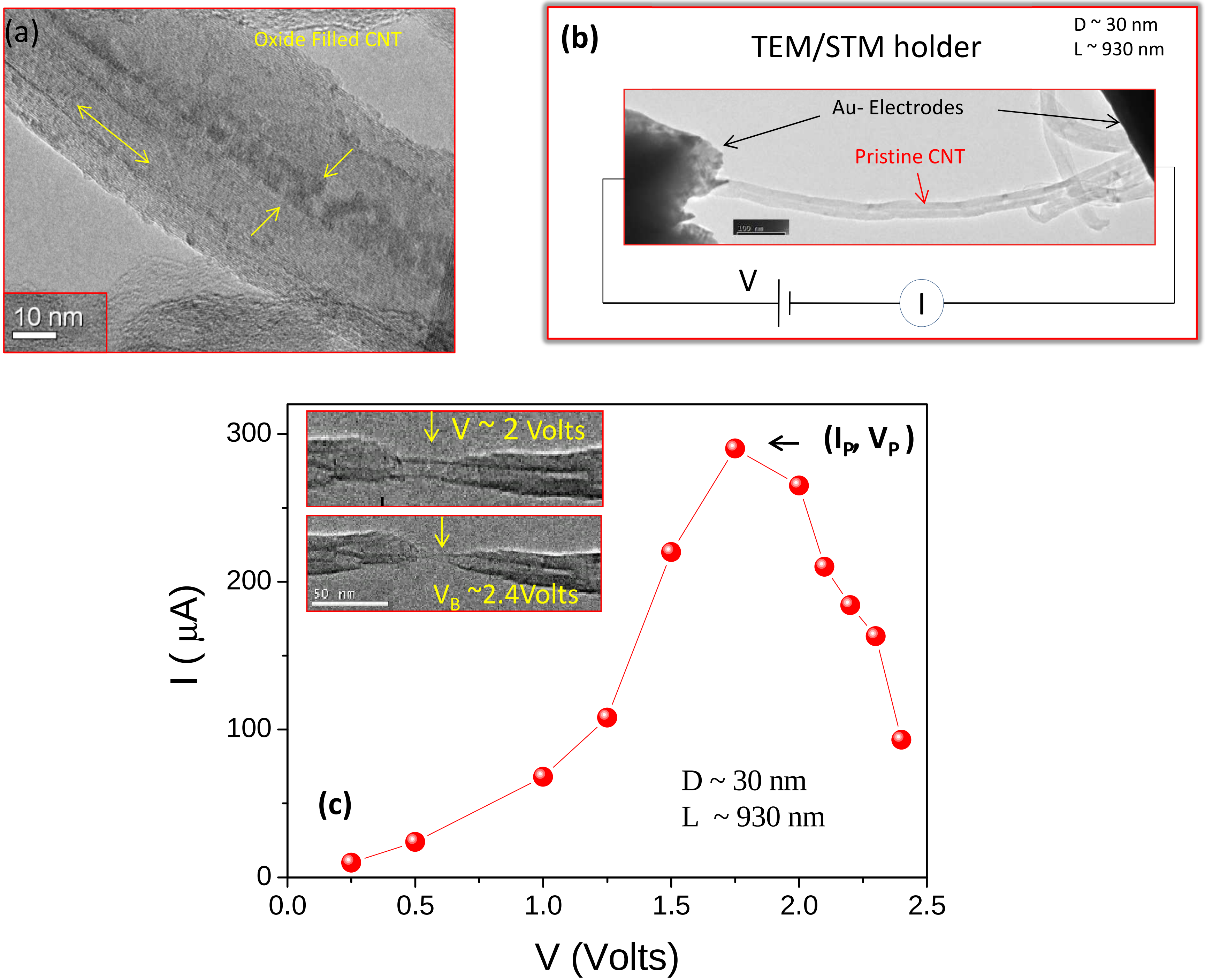

(a)
Oxide Filled CNT
10 nm
(b)
TEM/STM holder
D ~ 30 nm
L ~ 930 nm
Au- Electrodes
Pristine CNT
V
I
(c)
V ~ 2 Volts
V_B ~2.4Volts
50 nm
(I_P, V_P)
D ~ 30 nm
L ~ 930 nm
I (μA)
V (Volts)
0
100
200
300
0.0
0.5
1.0
1.5
2.0
2.5

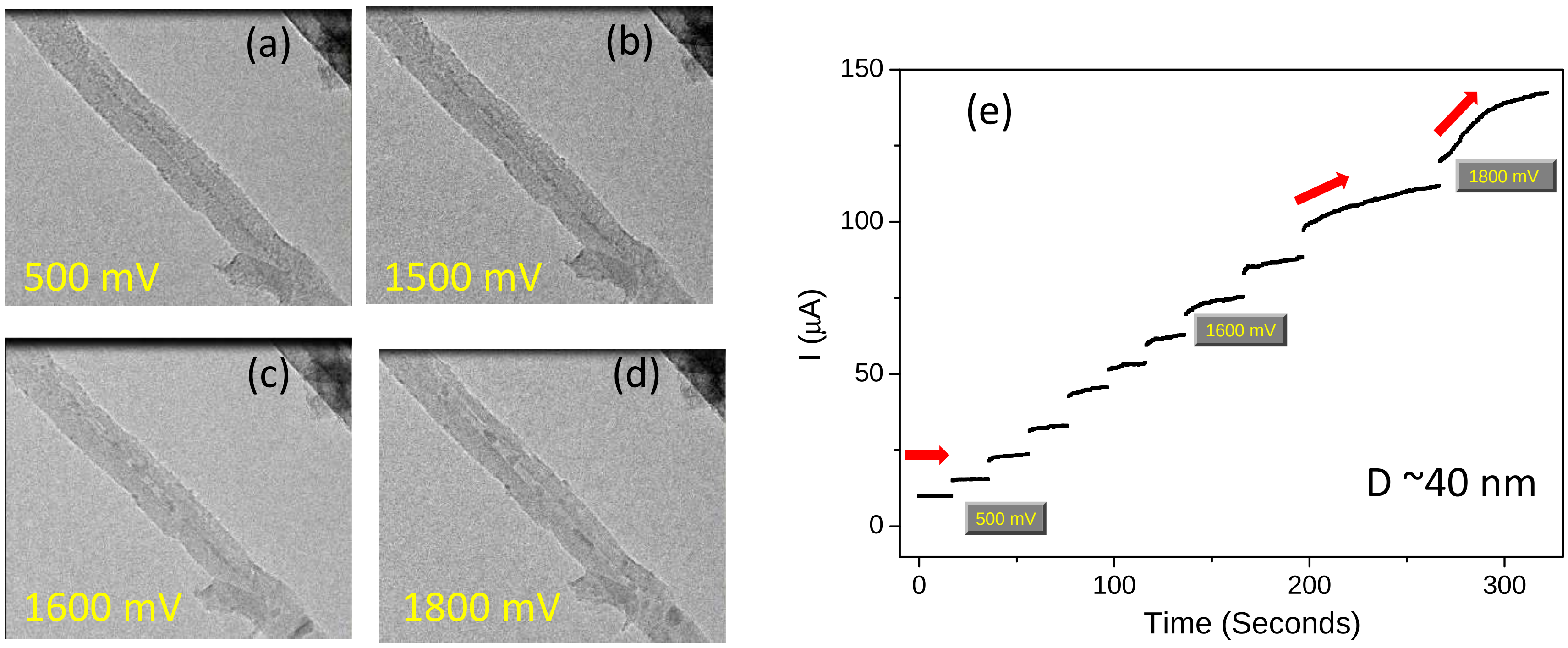
(a)
500 mV
(b)
1500 mV
(c)
1600 mV
(d)
1800 mV
(e)
I (µA)
Time (Seconds)
500 mV
1600 mV
1800 mV
D ~40 nm
0
50
100
150
0
100
200
300

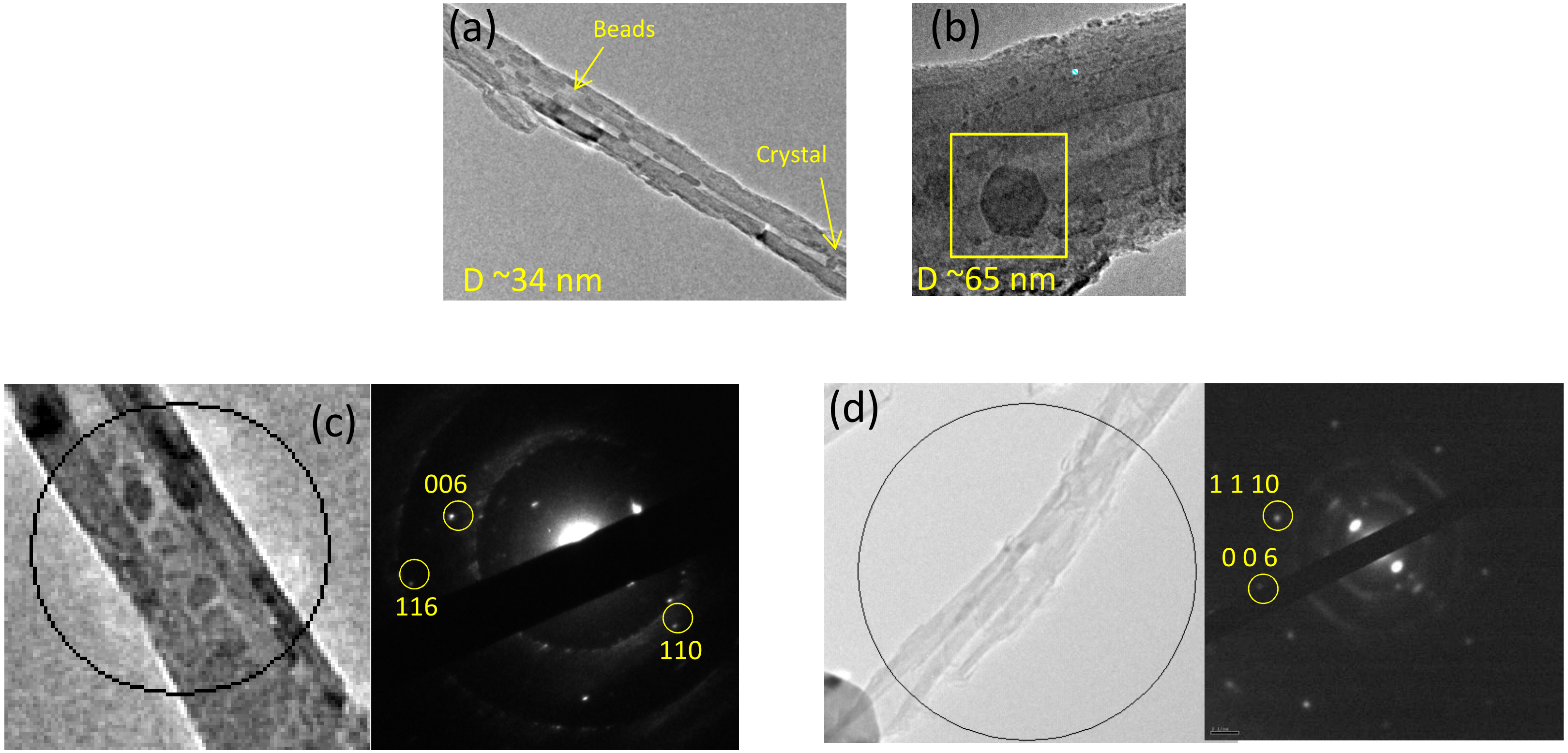
(a)
Beads
Crystal
D ~34 nm
(b)
D ~65 nm
(c)
006
116
110
(d)
1 1 10
0 0 6

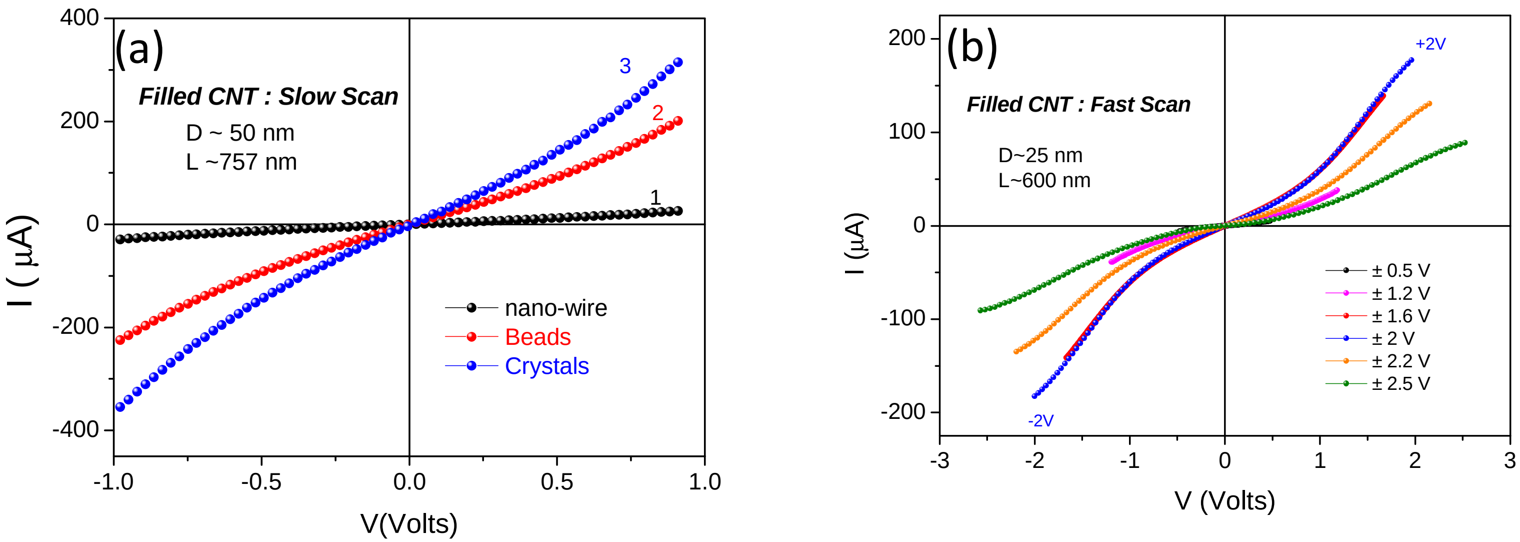
(a)
Filled CNT : Slow Scan
D ~ 50 nm
L ~757 nm
1
2
3
nano-wire
Beads
Crystals
I (μA)
V(Volts)
400
200
0
-200
-400
-1.0
-0.5
0.0
0.5
1.0
(b)
Filled CNT : Fast Scan
D~25 nm
L~600 nm
+2V
-2V
± 0.5 V
± 1.2 V
± 1.6 V
± 2 V
± 2.2 V
± 2.5 V
I (μA)
V (Volts)
200
100
0
-100
-200
-3
-2
-1
0
1
2
3

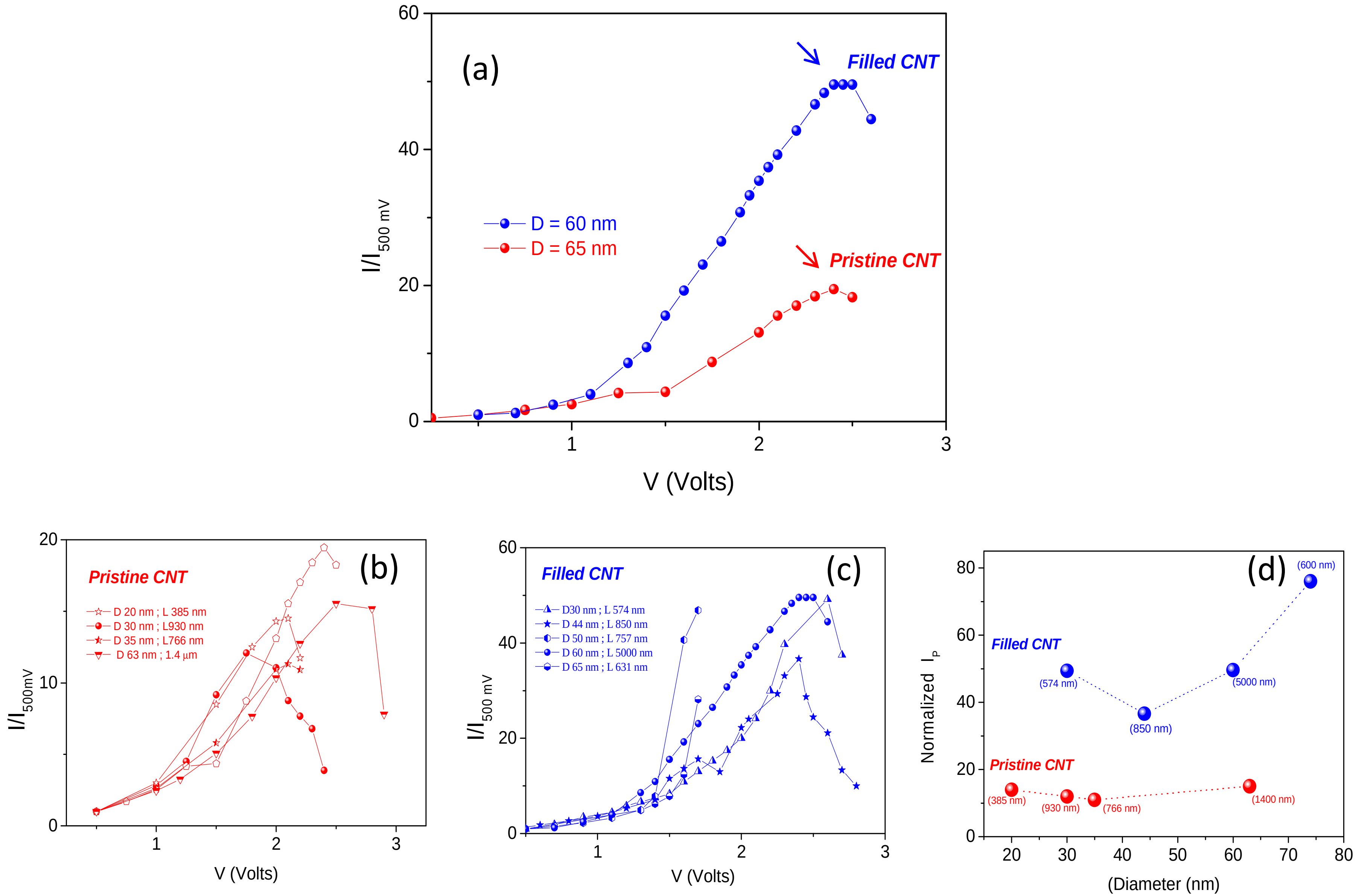

(a)
Filled CNT
Pristine CNT
D = 60 nm
D = 65 nm
I/I500 mV
V (Volts)
(b)
Pristine CNT
D 20 nm ; L 385 nm
D 30 nm ; L930 nm
D 35 nm ; L766 nm
D 63 nm ; 1.4 µm
I/I500mV
V (Volts)
(c)
Filled CNT
D30 nm ; L 574 nm
D 44 nm ; L 850 nm
D 50 nm ; L 757 nm
D 60 nm ; L 5000 nm
D 65 nm ; L 631 nm
I/I500 mV
V (Volts)
(d)
Filled CNT
Pristine CNT
(600 nm)
(574 nm)
(850 nm)
(5000 nm)
(385 nm)
(930 nm)
(766 nm)
(1400 nm)
Normalized Ip
(Diameter (nm))

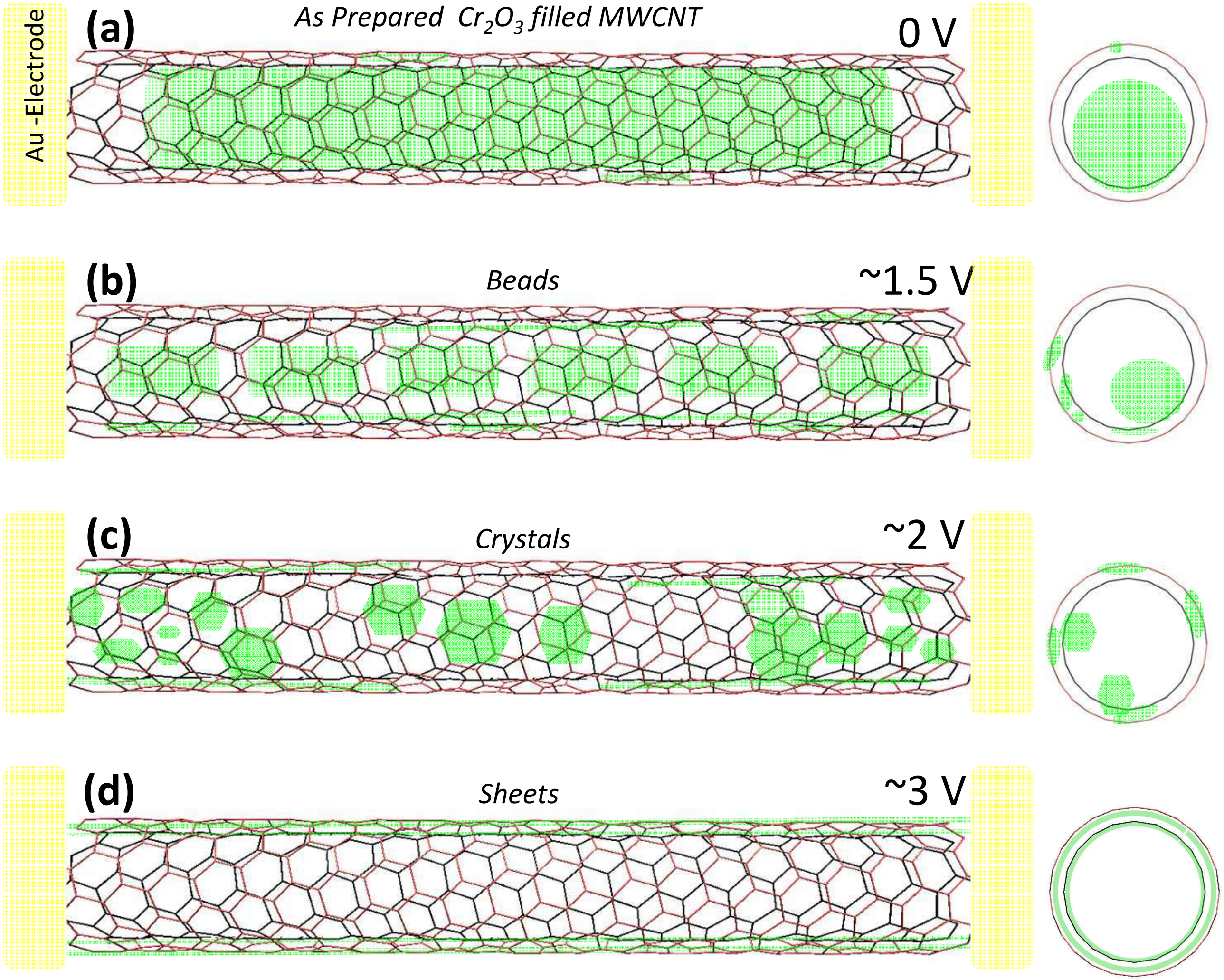
Au -Electrode
(a)
As Prepared Cr_2O_3 filled MWCNT
0 V
(b)
Beads
~1.5 V
(c)
Crystals
~2 V
(d)
Sheets
~3 V

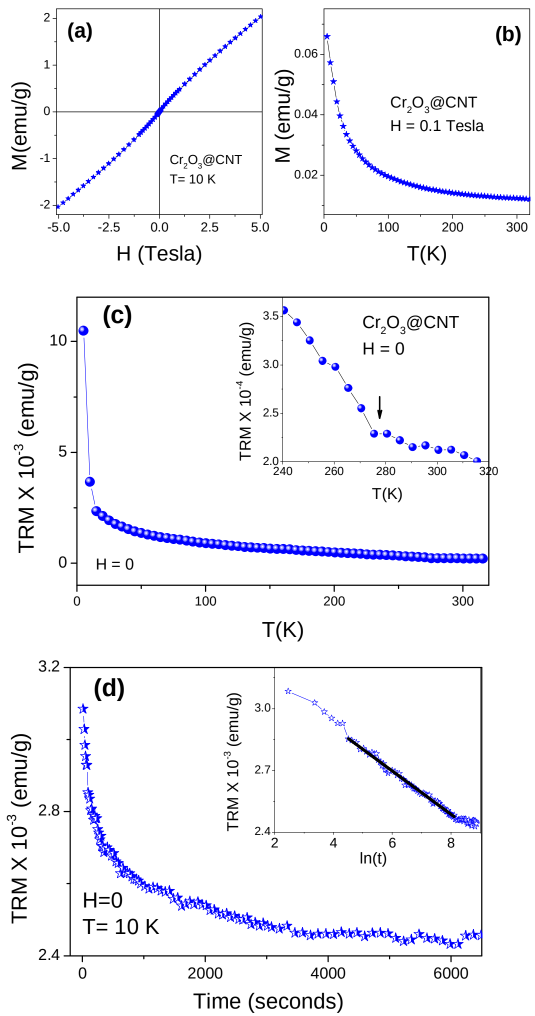
(a)
M(emu/g)
H (Tesla)
Cr2O3@CNT
T= 10 K
(b)
M (emu/g)
T(K)
Cr2O3@CNT
H = 0.1 Tesla
(c)
TRM X 10-3 (emu/g)
T(K)
H = 0
Cr2O3@CNT
H = 0
TRM X 10-4 (emu/g)
T(K)
(d)
TRM X 10-3 (emu/g)
Time (seconds)
H=0
T= 10 K
TRM X 10-3 (emu/g)
ln(t)